Global projections of intense tropical cyclone activity for the late 21st century from dynamical downscaling of CMIP5/RCP4.5 scenarios

Thomas R. Knutson[1], Joseph J. Sirutis[1], Ming Zhao[1], Robert E. Tuleya[2], Morris Bender[1], Gabriel A. Vecchi[1], Gabriele Villarini[3], and Daniel Chavas[4]

[1]Geophysical Fluid Dynamics Laboratory/NOAA, Princeton, NJ 08542

[2]Center for Coastal Physical Oceanography, Old Dominion University, Norfolk, VA 23508

[3] IIHR-Hydroscience & Engineering, The University of Iowa, Iowa City, IA

[4]Department of Civil and Environmental Engineering, Princeton University, Princeton, NJ

Apr. 15, 2015

Abstract.

Global projections of intense tropical cyclone activity are derived from the Geophysical Fluid Dynamics Laboratory (GFDL) HiRAM (50 km grid) atmospheric model and the GFDL Hurricane Model using a two-stage downscaling procedure. First, tropical cyclone genesis is simulated globally using the HiRAM atmospheric model. Each storm is then downscaled into the GFDL Hurricane Model, with horizontal grid-spacing near the storm of 6 km, and including ocean coupling (e.g., 'cold wake' generation). Simulations are performed using observed sea surface temperatures (SSTs) (1980-2008); for a "control run" with 20 repeating seasonal cycles; and for a late 21st century projection using an altered SST seasonal cycle obtained from a CMIP5/RCP4.5 multi-model ensemble. In general agreement with most previous studies, projections with this framework indicate fewer tropical cyclones globally in a warmer late-21st-century climate, but also an increase in average cyclone intensity, precipitation rates, and in the number and occurrence-days of very intense category 4-5 storms. While these changes are apparent in the globally averaged tropical cyclone statistics, they are not necessarily present in each individual basin. The inter-basin variation of changes in most of the tropical cyclone metrics we examined is directly correlated to the variation in magnitude of SST increases between the basins. Finally, the framework is shown capable of reproducing both the observed global distribution of outer storm size--albeit with a slight high bias--and its inter-basin variability. Projected median size is found to remain nearly constant globally, with increases in most basins offset by decreases in the Northwest Pacific.

Fig. 1

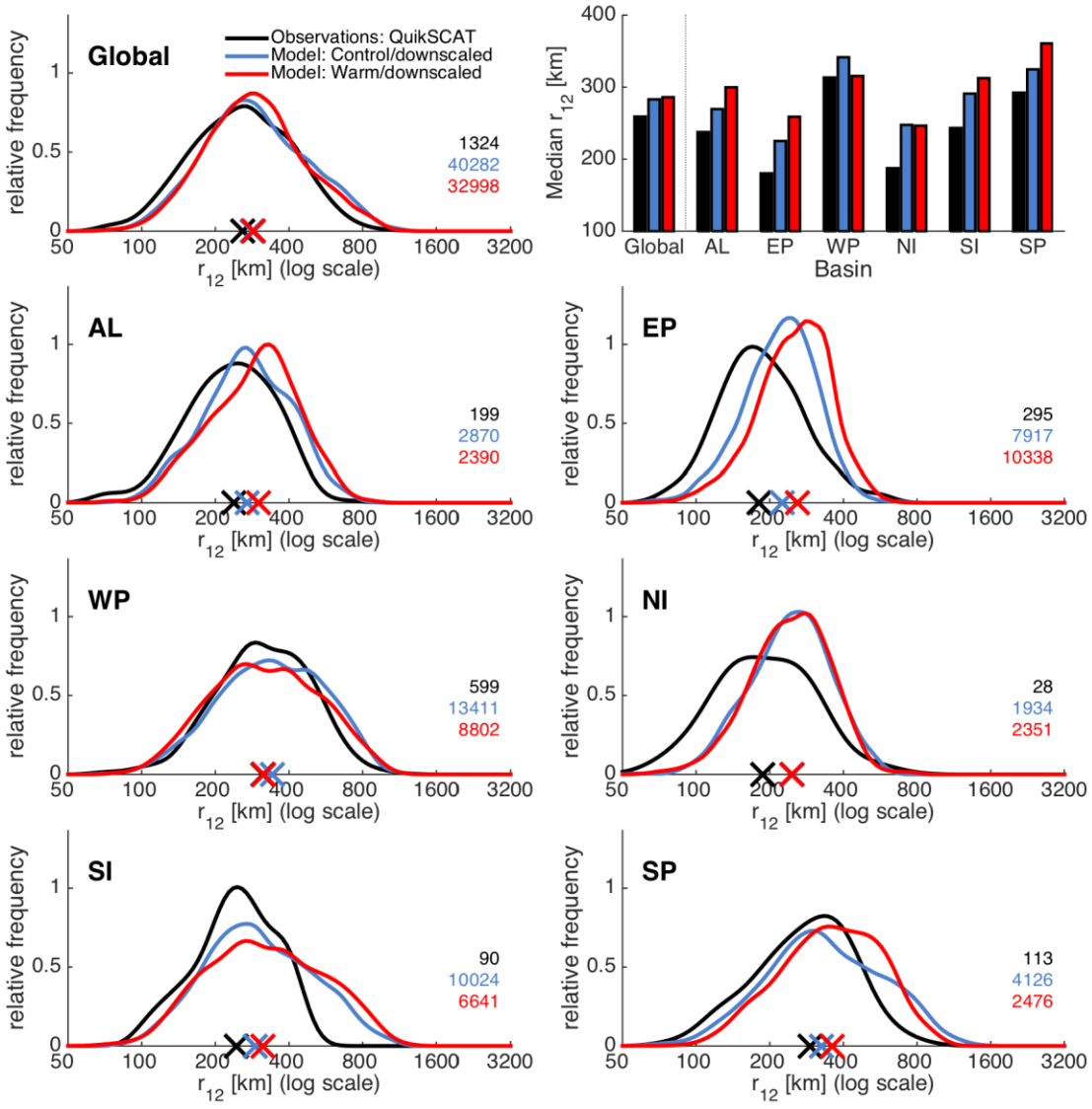

Fig. 1. Relative frequency of tropical cyclone size, globally (top left) and for various tropical cyclone basins (AL=North Atlantic; EP=Northeast Pacific; WP=Northwest Pacific; NI=North Indian; SI=South Indian; and SP=Southwest Pacific). The size metric, r_{12}, is the radius at which the azimuthally averaged windspeed decreases to 12 m s^{-1}. Black curves depict observed estimates based on QuikSCAT satellite measurements; blue and red curves depict distributions based on model simulations for control (present-day; blue) or warm climate (late 21st century; red) conditions. 'X' marks on each diagram denote median values. The numbers listed on each diagram denote the number of cases analyzed. Upper right: global and inter-basin variation of median tropical cyclone sizes for this metric. Control runs are based on climatological SSTs for 1982-2005.

Fig. 2

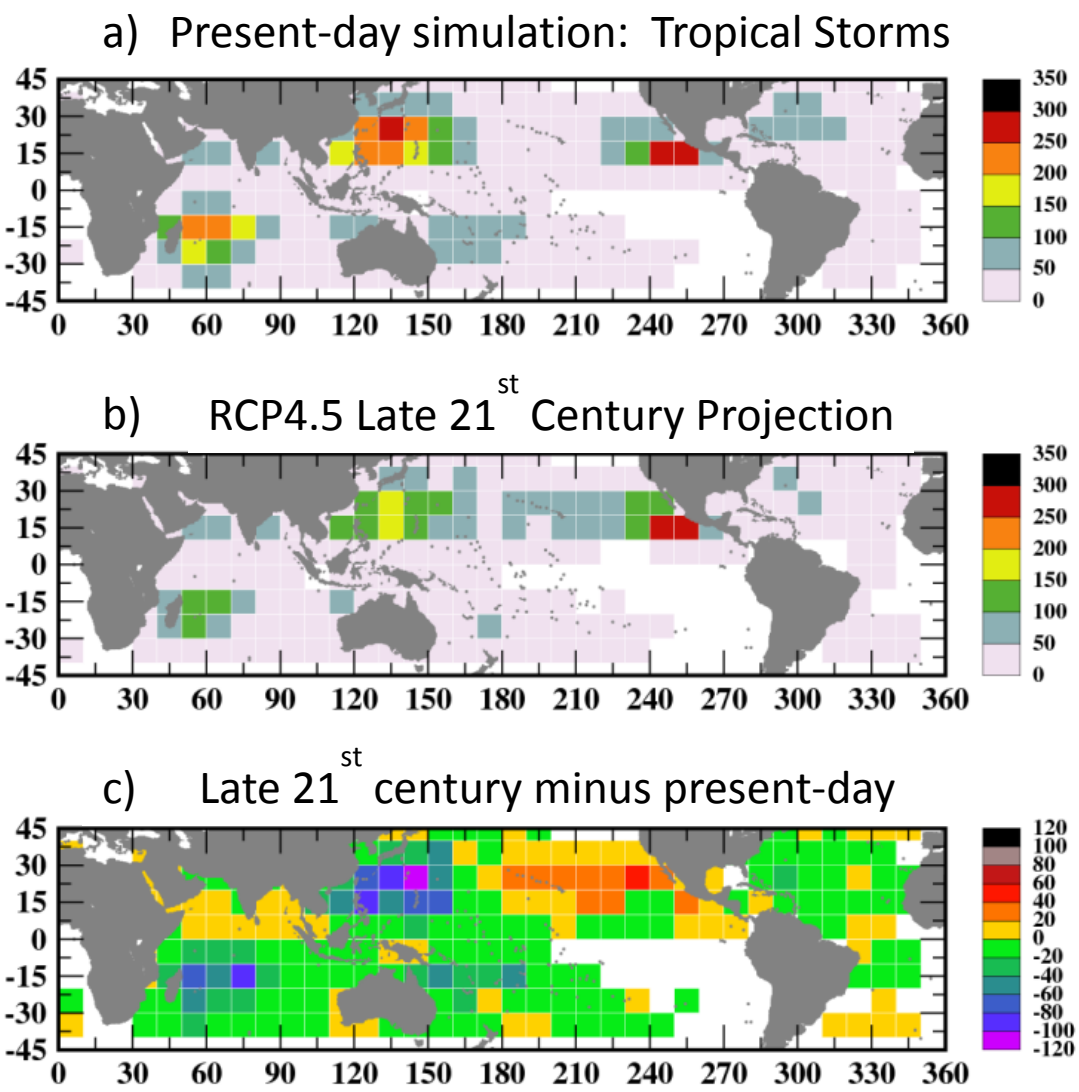

Fig. 2. Simulated occurrence of all tropical storms (tropical cyclones with winds exceeding 17.5 m s^{-1}) for: a) present-day or b) late 21st century (RCP4.5; CMIP5 multimodel ensemble) conditions; unit: storms per decade. Simulated tropical cyclone tracks were obtained using the GFDL Hurricane model to re-simulate (at higher resolution) the tropical cyclone cases originally obtained from the HiRAM C180 global mode. Occurrence refers to the number of days, over a 20 year period, in which a storm exceeding 17.5 m s^{-1} intensity was centered within the 10^{o}x10^{o} grid region. c) Difference in occurrence rate between late 21st century and present day, ((b) minus (a)). White regions are regions where no tropical storms occurred in the simulations (a,b) or where the difference between the experiments is zero (c).

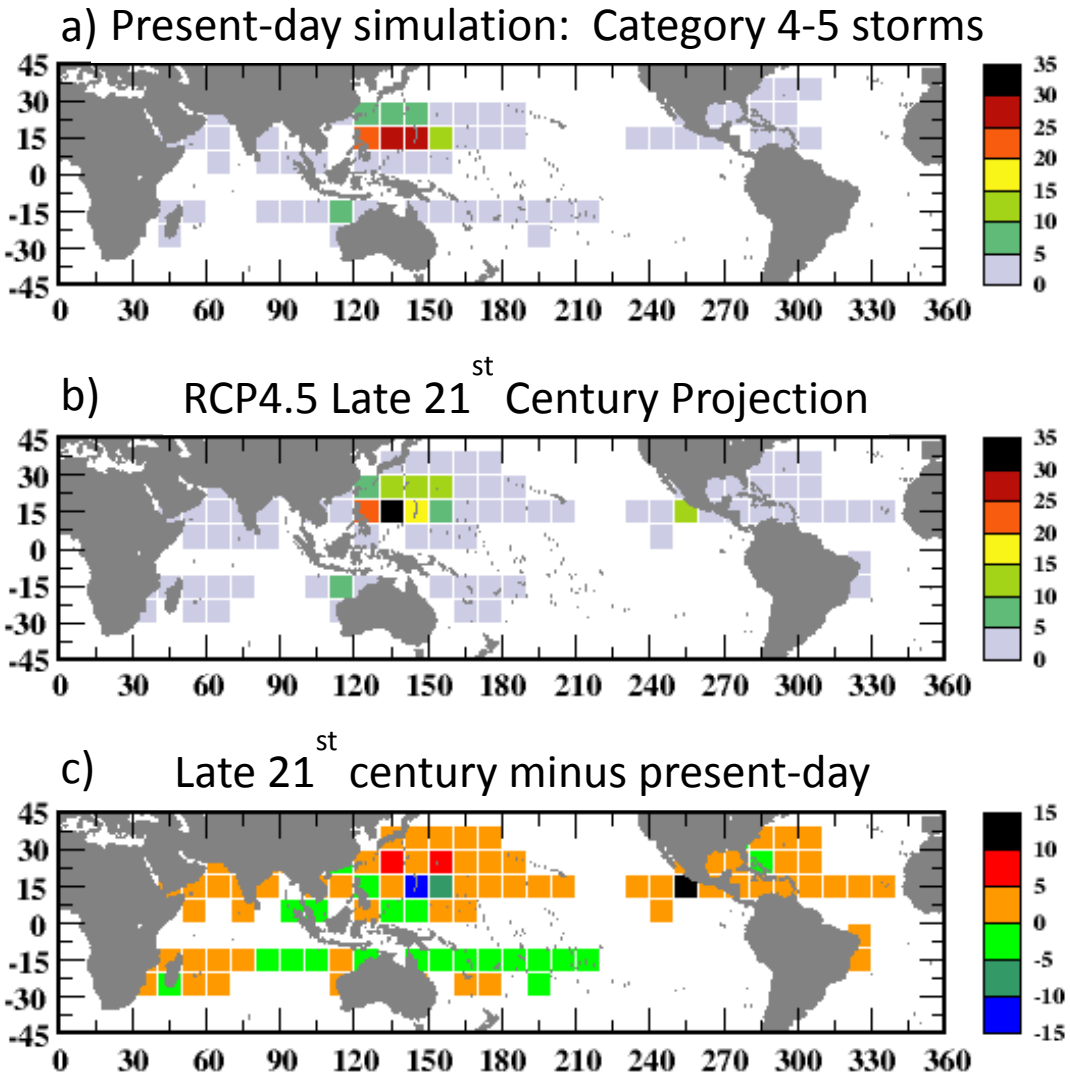

Fig. 3. As in Fig. 2 but for tropical cyclones of at least Category 4 intensity (surface winds of at least 59 m s^{-1}).

Fig. 4

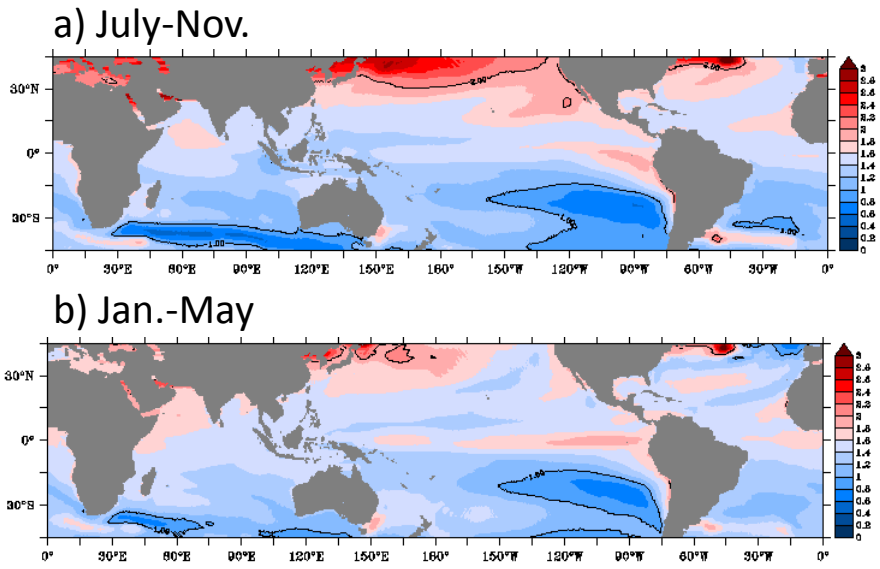

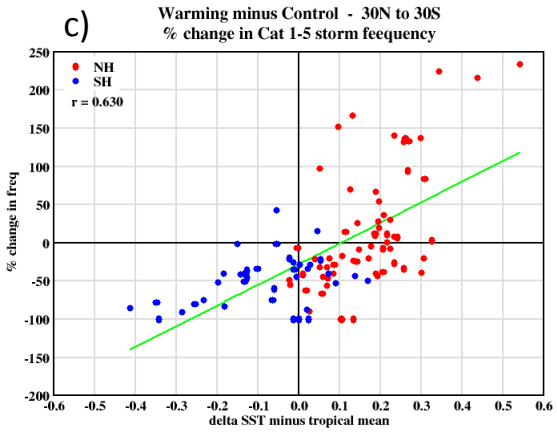

Fig. 4. SST difference (CMIP5/RCP4.5 late 21st century minus present day) used in the tropical cyclone dynamical downscaling experiments for the (a) July-November or (b) January-May seasons (units: ^{o}C). c) Scatterplot of percent change in hurricane (Category 1-5) occurrence frequency vs. SST difference for each 10^{o}x10^{o} grid box (30^{o}N-30^{o}S) that had nonzero hurricane occurrence in both control and warm climate simulations. SST differences are from (a) for all northern hemisphere basin points (red) and from (b) for all southern hemisphere basin points (blue) shown in (c).

Fig. 5

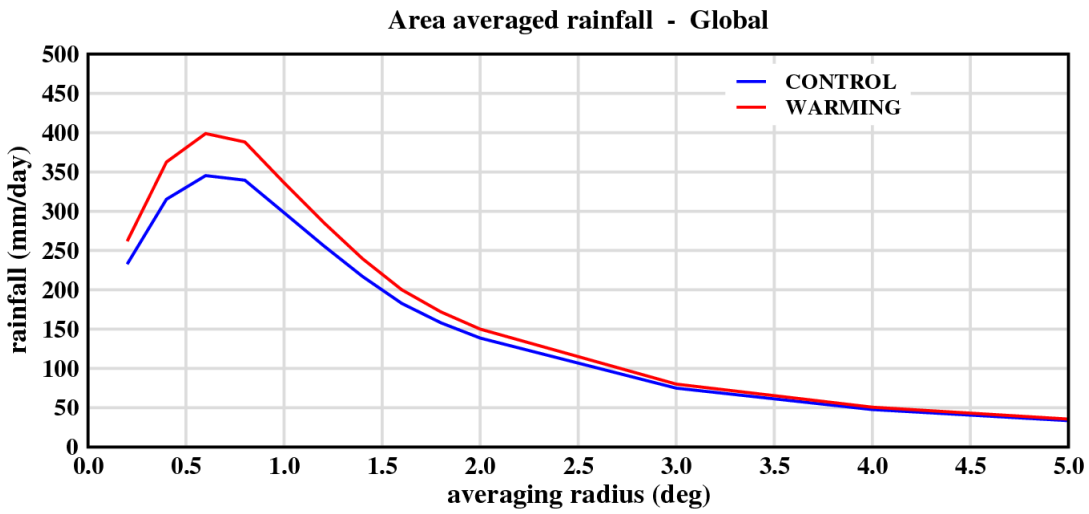

Fig. 5. Profiles of tropical cyclone precipitation rates (mm day^{-1}), for the 10% rainiest tropical cyclones (30^{o}N-30^{o}S) for the control runs (present-day; blue curve) or the warming runs (late 21st century RCP4.5 projection; red curve).

Fig. 6

a) Global

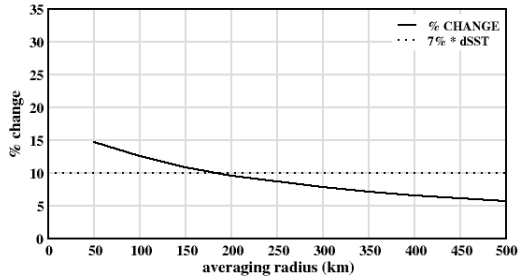

b) North Atlantic

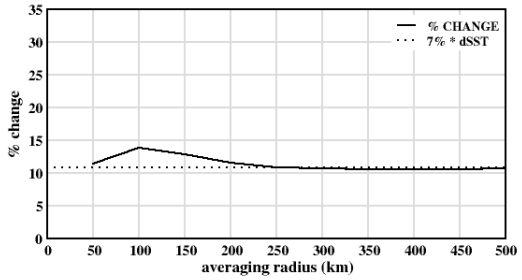

c) Northeast Pacific

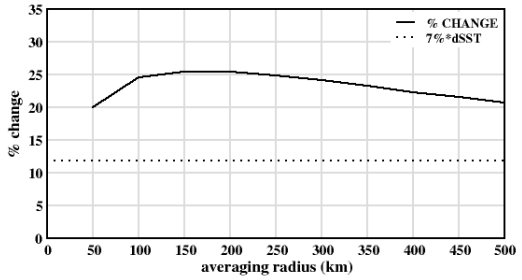

d) Northwest Pacific

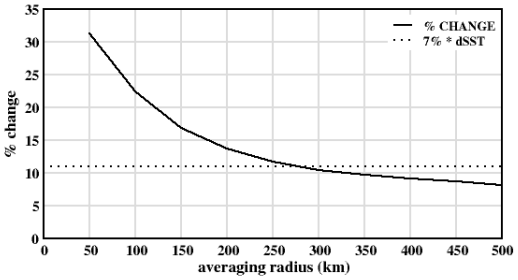

e) North Indian Ocean

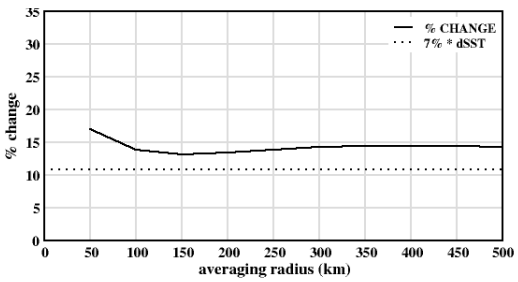

f) South Indian Ocean

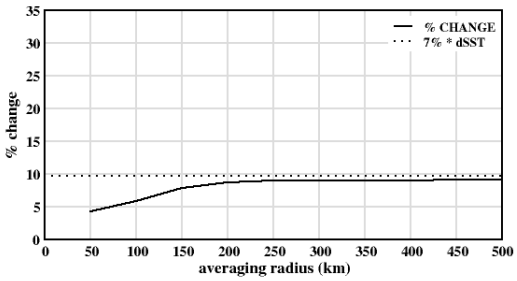

g) Southwest Pacific

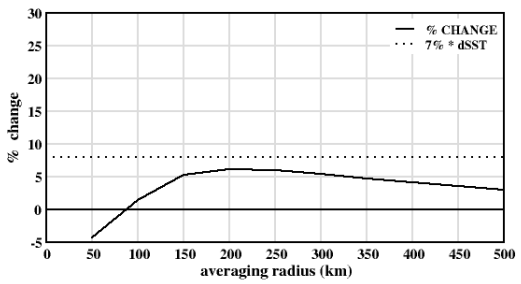

Fig. 6. Percent change (warm climate minus control) in tropical cyclone precipitation as a function of averaging radius from the storm center, for all tropical cyclones in each basin (a-g). The dotted line, computed as the SST change over the basin multiplied by 7% per ^{o}C, approximates the increase in atmospheric water vapor content in the basin associated with the SST warming, assuming negligible change in relative humidity.